Journal of Computational and Applied Mathematics 406 (2022) 114017

Contents lists available at ScienceDirect

Journal of Computational and Applied Mathematics

journal homepage: www.elsevier.com/locate/cam

# An iteration solver for the Poisson–Nernst–Planck system and its convergence analysis

Chun Liu [a], Cheng Wang [b,*], Steven M. Wise [c], Xingye Yue [d], Shenggao Zhou [e]

[a] Department of Applied Mathematics, Illinois Institute of Technology, IL 60616, USA
[b] Department of Mathematics, University of Massachusetts, North Dartmouth, MA 02747, USA
[c] Department of Mathematics, The University of Tennessee, Knoxville, TN 37996, USA
[d] Department of Mathematics, Soochow University, Suzhou 215006, China
[e] School of Mathematical Sciences and MOE-LSC, Shanghai Jiao Tong University, Shanghai, 200240, China

ARTICLE INFO

*Article history:*
Received 6 June 2021
Received in revised form 11 October 2021

*MSC:*
35K35
35K55
49J40
65M06
65M12

*Keywords:*
Poisson-Nernst–Planck (PNP) system
Logarithmic energy potential
Positivity preserving
Optimal rate convergence analysis
Modified Newton iteration
Linear convergence rate

ABSTRACT

In this paper, we provide a theoretical analysis for an iteration solver to implement a finite difference numerical scheme for the Poisson-Nernst–Planck (PNP) system, based on the Energetic Variational Approach (EnVarA), in which a non-constant mobility $H^{-1}$ gradient flow is formulated. In particular, the nonlinear and singular nature of the logarithmic energy potentials has always been the essential difficulty. In the numerical design, the mobility function is explicitly updated, for the sake of unique solvability analysis. The logarithmic and the electric potential diffusion terms, which come from the gradient of convex energy functional parts, are implicitly computed. The positivity-preserving property for all the concentrations, an unconditional energy stability, and the optimal rate error estimate have been established in a recent work. A modified Newton iteration for the nonlinear and logarithmic part, combined with a linear iteration for the electric potential part, is proposed to implement the given numerical scheme, in which a non-constant linear elliptic equation needs to be solved at each iteration stage. A theoretical analysis is presented in this article, and a linear convergence is proved for such an iteration, with an asymptotic error constant in the same order of the time step size. A numerical test is also presented in this article, which demonstrates the linear convergence rate of the proposed iteration solver.



## 1. Introduction

The Poisson-Nernst–Planck (PNP) system is formulated as

$$\partial_t n = D_n \Delta n - \frac{z_0 e_0}{k_B \theta_0} \nabla \cdot (D_n n \nabla \phi), \tag{1.1}$$

$$\partial_t p = D_p \Delta p + \frac{z_0 e_0}{k_B \theta_0} \nabla \cdot \left(D_p p \nabla \phi\right), \tag{1.2}$$

$$-\varepsilon \Delta \phi = z_0 e_0 (p - n) + \rho^f, \tag{1.3}$$

* Corresponding author.
*E-mail addresses:* cliu124@iit.edu (C. Liu), cwang1@umassd.edu (C. Wang), swise1@utk.edu (S.M. Wise), xyyue@suda.edu.cn (X. Yue), sgzhou@sjtu.edu.cn (S. Zhou).

https://doi.org/10.1016/j.cam.2021.114017
0377-0427/

where $n$ and $p$ are the concentrations of negatively and positively charged ions, and $\phi$ is the electric potential. In this model, $k_B, \theta_0, \varepsilon, z_0, e_0$ stand for the Boltzmann constant, the absolute temperature, the dielectric coefficient, valence of ions, the charge of an electron, respectively; the parameters $D_n$ and $D_p$ are diffusion/mobility coefficients. The periodic boundary conditions are assumed in this paper, for simplicity of presentation, and the presented analysis could be extended to more complicated, more physical boundary conditions, such as the homogeneous Neumann one. Furthermore, the source term $\rho^f$ is assumed to vanish everywhere, i.e., $\rho^f \equiv 0$. An extension to a non-homogeneous source term is straightforward. See the related works [1–6] for more detailed descriptions of this physical model.

In particular, the Energetic Variational Approach (EnVarA) [7] for the PNP system has attracted more and more attentions, since the PDE system is formulated as a gradient flow with respect to certain free energy. This framework has provided great convenience in the structure preserving analysis, at both the PDE and numerical levels. In fact, the dimensionless dynamical equations of the PNP system could be rewritten as (see the detailed derivation in [8])

$$\partial_t n = \nabla \cdot (\nabla n - n \nabla \phi), \tag{1.4}$$

$$\partial_t p = D \nabla \cdot (\nabla p + p \nabla \phi), \tag{1.5}$$

$$-\Delta \phi = p - n. \tag{1.6}$$

In fact, the parameter $D$ plays the role of a non-dimensional relative mobility. The corresponding dimensionless energy is given by

$$E(n, p) = \int_\Omega \{n \ln n + p \ln p\}\, d\mathbf{x} + \frac{1}{2} \|n - p\|_{H^{-1}}^2, \tag{1.7}$$

under the assumption that $n - p$ is of mean zero, and the $H^{-1}$ norm is defined via

$$\|f\|_{H^{-1}} := \sqrt{(f, f)_{H^{-1}}}, \quad (f, g) = (f, (-\Delta)^{-1} g) = ((-\Delta)^{-1} f, g), \quad \text{for } f \text{ and } g \text{ with mean zero.}$$

In turn, the PNP system (1.4)–(1.6) could be rewritten as the following conserved $H^{-1}$ gradient flow, with non-constant mobility:

$$\partial_t n = \nabla \cdot (n \nabla \mu_n), \quad \partial_t p = D \nabla \cdot \left(p \nabla \mu_p\right), \tag{1.8}$$

$$\mu_n := \delta_n E = \ln n + 1 + (-\Delta)^{-1}(n - p) = \ln n + 1 - \phi, \tag{1.9}$$

$$\mu_p := \delta_p E = \ln p + 1 + (-\Delta)^{-1}(p - n) = \ln p + 1 + \phi, \tag{1.10}$$

in which the electric potential is defined as $\phi = (-\Delta)^{-1}(p - n)$. A careful calculation implies that the energy dissipation law becomes $E'(t) = -\int_\Omega \left\{ n \left|\nabla \mu_n\right|^2 + D\, p \left|\nabla \mu_p\right|^2 \right\} d\mathbf{x} \le 0$.

Among the existing numerical works for the PNP system, the theoretical analysis for the positivity-preserving property, energy stability and convergence analysis turns out to be very challenging, due to the nonlinear and singular nature of the logarithmic terms in the EnVarA formulation. Some progresses have been made in recent years, such as the positivity-preserving analysis reported in [4,9–16], the energy stability analysis in [17–19], the convergence analysis in [20–23], as well as a few other related works [19,24–28]. In particular, a finite difference numerical scheme was proposed in [8], so that all three theoretical features have been established in the numerical analysis. In more details, the numerical scheme is based on the variational structure of the original PNP system, so that the energy stability analysis could be formulated in an appropriate framework. The mobility concentration function is explicitly updated in the scheme, for the sake of unique solvability analysis. In the chemical potential expansion, all the terms are implicitly computed, which comes from the convexity of both the logarithmic energy functional and the electric energy potential. The positivity-preserving property has been theoretically established for both ion concentration variables, with the help of the singularity feature of the logarithmic term, combined with its convex nature. In fact, similar techniques have been successfully applied to other gradient models with singular energy potential [29–36], etc. The energy stability is a direct consequence of the convexity analysis. In addition, an optimal rate convergence analysis for the proposed numerical scheme has been reported in [8], based on an asymptotic expansion for the numerical solution, combined with rough error estimate and refined error estimate.

On the other hand, this numerical scheme is highly nonlinear and singular, due to the implicit treatment of the singular logarithmic chemical potential parts. In addition, an implicit treatment of the electric part leads to a highly coupled numerical system. These facts make the proposed numerical scheme very challenging to implement. In this article, we propose and analyze an iteration solver for this numerical scheme. A linearized Newton iteration is applied to the nonlinear and singular logarithmic parts, while a linear iteration is used for the electric potential part. In turn, a divergence-form elliptic system needs to be solved at each iteration stage, which in turn leads to a computational cost comparable to a standard Poisson solver. In addition, the positivity of both concentration variables at each iteration stage is crucial to ensure the well-posed property of the elliptic system. The convergence analysis will be provided for the proposed iteration algorithm, under the separation assumption for the exact PDE solution, i.e., a uniform distance is ensured between the exact PDE solution and the singular value of 0. With such an assumption for the exact PDE solution, a similar uniform distance could be derived for the numerical solution at each iteration stage, using an a-priori $\|\cdot\|_\infty$

error estimate for the iteration solution. With the help of this uniform distance, the singularity issue associated with the logarithmic term could be avoided in the iteration analysis. Moreover, the convex nature of the logarithmic energy functional will lead to a well-posed error analysis for the nonlinear part at each iteration stage. As a result of all these techniques, a linear convergence analysis is reported for the proposed iteration process, with the convergence rate in the same order of the time step size. In our knowledge, it will be the first such result for the highly nonlinear and singular PNP system.

The rest of the article is organized as follows. In Section 2 the numerical scheme is reviewed, and the main theoretical results are recalled, if the numerical solution could be exactly implemented. In turn, the iteration solver is introduced in Section 3, and a linear convergence analysis is provided in details. A numerical test is presented in Section 4, and the linear convergence rate of the proposed iteration solver is confirmed in the test. Finally, some concluding remarks are given in Section 5.

## 2. Review of the numerical scheme

### 2.1. The finite difference spatial discretization

The standard centered finite difference spatial approximation is applied. We present the numerical approximation on the computational domain $\Omega = (0, 1)^3$ with a periodic boundary condition, and $\Delta x = \Delta y = \Delta z = h = \frac{1}{N}$ with $N \in \mathbb{N}$ to be the spatial mesh resolution throughout this work. In particular, $f_{i,j,k}$ stands for the numerical value of $f$ at the cell centered mesh points $((i+\frac{1}{2})h, (j+\frac{1}{2})h, (k+\frac{1}{2})h)$, and we denote $\mathcal{C}_{\rm per}$ as

$$\mathcal{C}_{\rm per} := \left\{ (f_{i,j,k}) \,|\, f_{i,j,k} = f_{i+\alpha N, j+\beta N, k+\gamma N},\ \forall\, i,j,k,\alpha,\beta,\gamma \in \mathbb{Z} \right\},$$

with the discrete periodic boundary condition imposed. In turn, the discrete average and difference operators are evaluated at $((i+1)h, (j+\frac{1}{2})h, (k+\frac{1}{2})h)$, $((i+\frac{1}{2})h, (j+1)h, (k+\frac{1}{2})h)$ and $((i+\frac{1}{2})h, (j+\frac{1}{2})h, (k+1)h)$, respectively:

$$\begin{aligned}
&A_x f_{i+1/2,j,k} := \frac{1}{2}\left(f_{i+1,j,k} + f_{i,j,k}\right), \quad D_x f_{i+1/2,j,k} := \frac{1}{h}\left(f_{i+1,j,k} - f_{i,j,k}\right),\\
&A_y f_{i,j+1/2,k} := \frac{1}{2}\left(f_{i,j+1,k} + f_{i,j,k}\right), \quad D_y f_{i,j+1/2,k} := \frac{1}{h}\left(f_{i,j+1,k} - f_{i,j,k}\right),\\
&A_z f_{i,j,k+1/2} := \frac{1}{2}\left(f_{i,j,k+1} + f_{i,j,k}\right), \quad D_z f_{i,j,k+1/2} := \frac{1}{h}\left(f_{i,j,k+1} - f_{i,j,k}\right).
\end{aligned}$$

Conversely, the corresponding operators at the staggered mesh points are defined as follows:

$$\begin{aligned}
&a_x f^x_{i,j,k} := \frac{1}{2}\left(f^x_{i+1/2,j,k} + f^x_{i-1/2,j,k}\right), \quad d_x f^x_{i,j,k} := \frac{1}{h}\left(f^x_{i+1/2,j,k} - f^x_{i-1/2,j,k}\right),\\
&a_y f^y_{i,j,k} := \frac{1}{2}\left(f^y_{i,j+1/2,k} + f^y_{i,j-1/2,k}\right), \quad d_y f^y_{i,j,k} := \frac{1}{h}\left(f^y_{i,j+1/2,k} - f^y_{i,j-1/2,k}\right),\\
&a_z f^z_{i,j,k} := \frac{1}{2}\left(f^z_{i,j,k+1/2} + f^z_{i,j,k-1/2}\right), \quad d_z f^z_{i,j,k} := \frac{1}{h}\left(f^z_{i,j,k+1/2} - f^z_{i,j,k-1/2}\right).
\end{aligned}$$

In turn, for a scalar cell-centered function $g$ and a vector function $\vec{f} = (f^x, f^y, f^z)^T$, with $f^x$, $f^y$ and $f^z$ evaluated at $((i+1)h, (j+\frac{1}{2})h, (k+\frac{1}{2})h)$, $((i+\frac{1}{2})h, (j+1)h, (k+\frac{1}{2})h)$, $((i+\frac{1}{2})h, (j+\frac{1}{2})h, (k+1)h)$, respectively, the discrete divergence is defined as

$$\nabla_h \cdot \left(g\vec{f}\right)_{i,j,k} = d_x\left(A_x g \cdot f^x\right)_{i,j,k} + d_y\left(A_y g \cdot f^y\right)_{i,j,k} + d_z\left(A_z g \cdot f^z\right)_{i,j,k}. \tag{2.1}$$

In particular, if $\vec{f} = \nabla_h \phi = (D_x\phi, D_y\phi, D_z\phi)^T$ for certain scalar grid function $\phi$, the corresponding divergence becomes

$$\nabla_h \cdot \left(g\nabla_h\phi\right)_{i,j,k} = d_x\left(A_x g \cdot D_x\phi\right)_{i,j,k} + d_y\left(A_y g \cdot D_y\phi\right)_{i,j,k} + d_z\left(A_z g \cdot D_z\phi\right)_{i,j,k}, \tag{2.2}$$

$$\left(\Delta_h\phi\right)_{i,j,k} = \nabla_h \cdot \left(\nabla_h\phi\right)_{i,j,k} = d_x\left(D_x\phi\right)_{i,j,k} + d_y\left(D_y\phi\right)_{i,j,k} + d_z\left(D_z\phi\right)_{i,j,k}. \tag{2.3}$$

For two cell-centered grid functions $f$ and $g$, its discrete $L^2$ inner product and the associated $\ell^2$ norm are defined as

$$\langle f, g\rangle_\Omega := h^3 \sum_{i,j,k=1}^{N} f_{i,j,k} g_{i,j,k}, \quad \|f\|_2 := \left(\langle f, f\rangle_\Omega\right)^{\frac{1}{2}}.$$

In turn, the mean zero space is introduced as $\mathring{\mathcal{C}}_{\rm per} := \left\{ f \in \mathcal{C}_{\rm per} \,|\, 0 = \overline{f} := \frac{h^3}{|\Omega|}\sum_{i,j,k=1}^{m} f_{i,j,k} \right\}$. Similarly, for two vector grid functions $\vec{f} = (f^x, f^y, f^z)^T$, $\vec{g} = (g^x, g^y, g^z)^T$, with $f^x$ $(g^x)$, $f^y$ $(g^y)$, $f^z$ $(g^z)$ evaluated at $((i+1)h, (j+\frac{1}{2})h, (k+\frac{1}{2})h)$, $((i+\frac{1}{2})h, (j+1)h, (k+\frac{1}{2})h)$, $((i+\frac{1}{2})h, (j+\frac{1}{2})h, (k+1)h)$, respectively, the corresponding discrete inner product becomes

$$\begin{aligned}
&\left[\vec{f}, \vec{g}\right] := \left[f^x, g^x\right]_{\rm x} + \left[g^y, g^y\right]_{\rm y} + \left[f^z, g^z\right]_{\rm z},\\
&\left[f^x, g^x\right]_{\rm x} := \left\langle a_x(f^x g^x), 1\right\rangle, \quad \left[f^y, g^y\right]_{\rm y} := \left\langle a_y(f^y g^y), 1\right\rangle, \quad \left[f^z, g^z\right]_{\rm z} := \left\langle a_z(f^z g^z), 1\right\rangle.
\end{aligned}$$

In addition to the discrete $\|\cdot\|_2$ norm, the discrete maximum norm is defined as $\|f\|_\infty := \max_{1\le i,j,k\le N} |f_{i,j,k}|$. Moreover, the discrete $H_h^1$ and $H_h^2$ norms are introduced as

$$\|\nabla_h f\|_2^2 := [\nabla_h f, \nabla_h f] = [D_x f, D_x f]_x + [D_y f, D_y f]_y + [D_z f, D_z f]_z,$$
$$\|f\|_{H_h^1}^2 := \|f\|_2^2 + \|\nabla_h f\|_2^2, \quad \|f\|_{H_h^2}^2 := \|f\|_{H_h^1}^2 + \|\Delta_h f\|_2^2.$$

The summation by parts formulas are recalled in the following lemma; the detailed proof could be found in [37–40], etc.

**Lemma 2.1** *([37–40]). For any $\psi, \phi, g \in \mathcal{C}_{\rm per}$, and any $\vec{f} = (f^x, f^y, f_z)^T$, with $f^x, f^y, f^z$ evaluated at $((i+1)h, (j+\frac{1}{2})h, (k+\frac{1}{2})h)$, $((i+\frac{1}{2})h, (j+1)h, (k+\frac{1}{2})h)$, $((i+\frac{1}{2})h, (j+\frac{1}{2})h, (k+1)h)$, respectively, the following summation by parts formulas are valid:*

$$\left\langle \psi, \nabla_h \cdot \vec{f} \right\rangle_\Omega = -\left[\nabla_h \psi, \vec{f}\right], \quad \langle \psi, \nabla_h \cdot (g \nabla_h \phi)\rangle_\Omega = -[\nabla_h \psi, \mathcal{A}_h g \nabla_h \phi], \tag{2.4}$$

*in which $\mathcal{A}_h$ corresponds to the average operator given by $A_x$, $A_y$ and $A_z$.*

In addition, a few notations need to be introduced, to facilitate the analysis in later sections. For any $\varphi \in \mathring{\mathcal{C}}_{\rm per}$ and a positive cell centered grid function $g$ (at a point-wise level), the weighed discrete norm is defined as

$$\|\varphi\|_{\mathcal{L}_g^{-1}} = \sqrt{\left\langle \varphi, \mathcal{L}_{\breve{\mathcal{M}}}^{-1}(\varphi)\right\rangle_\Omega}, \tag{2.5}$$

in which $\psi = \mathcal{L}_g^{-1}(\varphi) \in \mathring{\mathcal{C}}_{\rm per}$ is the unique solution that solves

$$\mathcal{L}_g(\psi) := -\nabla_h \cdot (g \nabla_h \psi) = \varphi. \tag{2.6}$$

In a simplified case of $g \equiv 1$, it is obvious that $\mathcal{L}_g(\psi) = -\Delta_h \psi$, and the discrete $H_h^{-1}$ inner product and $H_h^{-1}$ norm are introduced as $\langle \varphi_1, \varphi_2\rangle_{-1,h} = \langle \varphi_1, (-\Delta_h)^{-1}\varphi_2\rangle_\Omega$, and $\|\varphi\|_{-1,h} = \sqrt{\langle \varphi, (-\Delta_h)^{-1}\varphi\rangle_\Omega}$.

### 2.2. Review of the numerical scheme

The mobility function at the face-centered mesh points are defined as

$$(\breve{\mathcal{M}}_n^m)_{i+1/2,j,k} := A_x(\mathcal{M}_n^m)_{i+1/2,j,k},$$
$$(\breve{\mathcal{M}}_n^m)_{i,j+1/2,k} := A_y(\mathcal{M}_n^m)_{i,j+1/2,k}, \tag{2.7}$$
$$(\breve{\mathcal{M}}_n^m)_{i,j,k+1/2} := A_z(\mathcal{M}_n^m)_{i,j,k+1/2},$$

in which $(\mathcal{M}_n^m)_{i,j,k} = n_{i,j,k}^m$. Similar definitions could be introduced for $\breve{\mathcal{M}}_p^m$. The following finite difference scheme has been proposed in a recent work [8]: given $n^m, p^m \in \mathcal{C}_{\rm per}$, find $n^{m+1}, p^{m+1} \in \mathcal{C}_{\rm per}$ such that

$$\frac{n^{m+1} - n^m}{\Delta t} = \nabla_h \cdot \left(\breve{\mathcal{M}}_n^m \nabla_h \mu_n^{m+1}\right), \tag{2.8}$$
$$\frac{p^{m+1} - p^m}{\Delta t} = \nabla_h \cdot \left(\breve{\mathcal{M}}_p^m \nabla_h \mu_p^{m+1}\right), \tag{2.9}$$
$$\mu_n^{m+1} = \ln n^{m+1} + (-\Delta_h)^{-1}(n^{m+1} - p^{m+1}), \tag{2.10}$$
$$\mu_p^{m+1} = \ln p^{m+1} + (-\Delta_h)^{-1}(p^{m+1} - n^{m+1}). \tag{2.11}$$

### 2.3. The theoretical results for the proposed numerical scheme

It is observed that the numerical solution to (2.8)–(2.11) is mass conservative, i.e.,

$$\overline{n^m} = \overline{n^0} := \beta_0, \quad \overline{p^m} = \overline{p^0} := \beta_0, \quad \text{with} \quad 0 < \beta_0, \quad \forall\, m \ge 1, \tag{2.12}$$

in which the average operator is given by $\overline{f} = \frac{1}{|\Omega|}\langle f, \mathbf{1}\rangle_\Omega$.

**Lemma 2.2.** *Assume that the mobility function $\breve{\mathcal{M}}$ has uniform lower and upper bounds: $M_0 \le \breve{\mathcal{M}} \le M_1$. For any $g$ with $\overline{g} = 0$, we have*

$$\frac{M_0}{M_1^2}\|g\|_{-1,h}^2 \le \|g\|_{\mathcal{L}_{\breve{\mathcal{M}}}^{-1}}^2 \le \frac{M_1}{M_0^2}\|g\|_{-1,h}^2. \tag{2.13}$$

**Proof.** We denote $\psi$ as the solution to the non-constant elliptic equation, $-\nabla_h \cdot (\breve{\mathcal{M}} \nabla_h \psi_g) = g$, and $\varphi_g = (-\Delta_h)^{-1} g$, i.e., $-\Delta_h \varphi_g = g$. Taking a test function $\varphi_g$ with both equations $-\nabla_h \cdot (\breve{\mathcal{M}} \nabla_h \psi_g) = g$, $-\Delta_h \varphi_g = g$, respectively, we get

$$\langle \breve{\mathcal{M}} \nabla_h \psi_g, \nabla_h \varphi_g\rangle_\Omega = \langle g, \varphi_g\rangle_\Omega = \|\nabla_h \varphi_g\|_2^2. \tag{2.14}$$

Meanwhile, an application of Cauchy inequality implies that

$$\begin{aligned} &\|\nabla_h\varphi_g\|_2^2 = \langle \breve{\mathcal{M}}\nabla_h\psi_g, \nabla_h\varphi_g\rangle_\Omega \le M_1\|\nabla_h\psi_g\|_2\cdot\|\nabla_h\varphi_g\|_2, \\ &\text{which in turn gives}\quad \|\nabla_h\psi_g\|_2 \ge \frac{1}{M_1}\|\nabla_h\varphi_g\|_2. \end{aligned} \tag{2.15}$$

Similarly, taking a test function $\psi_g$ to both equations $-\nabla_h\cdot(\breve{\mathcal{M}}\nabla_h\psi_g) = g$, $-\Delta_h\varphi_g = g$, respectively, we get

$$\langle \breve{\mathcal{M}}\nabla_h\psi_g, \nabla_h\psi_g\rangle_\Omega = \langle g, \psi_g\rangle_\Omega = \langle \nabla_h\psi_g, \nabla_h\varphi_g\rangle_\Omega, \tag{2.16}$$

which in turn results in

$$\begin{aligned} &M_0\|\nabla_h\psi_g\|_2^2 \le \langle \breve{\mathcal{M}}\nabla_h\psi_g, \nabla_h\psi_g\rangle_\Omega = \langle \nabla_h\psi_g, \nabla_h\varphi_g\rangle_\Omega \le \|\nabla_h\psi_g\|_2\cdot\|\nabla_h\varphi_g\|_2, \\ &\text{so that}\quad \|\nabla_h\psi_g\|_2 \le \frac{1}{M_0}\|\nabla_h\varphi_g\|_2. \end{aligned} \tag{2.17}$$

Therefore, we arrive at

$$\begin{aligned} &\|g\|_{\mathcal{L}_{\breve{\mathcal{M}}}^{-1}}^2 = \langle \breve{\mathcal{M}}\nabla_h\psi_g, \nabla_h\psi_g\rangle_\Omega \le M_1\|\nabla_h\varphi_g\|_2^2 \le \frac{M_1}{M_0^2}\|g\|_{-1,h}^2, \\ &\|g\|_{\mathcal{L}_{\breve{\mathcal{M}}}^{-1}}^2 = \langle \breve{\mathcal{M}}\nabla_h\psi_g, \nabla_h\psi_g\rangle_\Omega \ge M_0\|\nabla_h\varphi_g\|_2^2 \ge \frac{M_0}{M_1^2}\|g\|_{-1,h}^2, \end{aligned} \tag{2.18}$$

in which the identity that $\|\nabla_h\varphi_g\|_2^2 = \|g\|_{-1,h}^2$ has been repeatedly applied. This finishes the proof of Lemma 2.2. □

The positivity-preserving and unique solvability properties are established in the following theorem.

**Theorem 2.1** ([8]). *Given $n^m, p^m \in \mathcal{C}_{\text{per}}$, with $0 < n_{i,j,k}^m, p_{i,j,k}^m$, $1 \le i,j,k \le N$, and $n^m - p^m \in \mathring{\mathcal{C}}_{\text{per}}$, there exists a unique solution $(n^{m+1}, p^{m+1}) \in \left[\mathcal{C}_{\text{per}}\right]^2$ to the numerical scheme (2.8)–(2.11), with $0 < n_{i,j,k}^{m+1}, p_{i,j,k}^{m+1}$, $1 \le i,j,k \le N$ and $n^{m+1} - p^{m+1} \in \mathring{\mathcal{C}}_{\text{per}}$.*

In terms of the energy stability analysis, the following discrete energy is introduced:

$$E_h(n,p) := \langle n\ln n + p\ln p, \mathbf{1}\rangle_\Omega + \frac{1}{2}\|n-p\|_{-1,h}^2. \tag{2.19}$$

**Theorem 2.2** ([8]). *For the numerical solution (2.8)–(2.11), we have*

$$E_h(n^{m+1}, p^{m+1}) + \Delta t\left(\left[\breve{\mathcal{M}}_n^m\nabla_h\mu_n^{m+1}, \nabla_h\mu_n^{m+1}\right] + \left[\breve{\mathcal{M}}_p^m\nabla_h\mu_p^{m+1}, \nabla_h\mu_p^{m+1}\right]\right) \le E_h(n^m, p^m), \tag{2.20}$$

*so that $E_h(n^m, p^m) \le E_h(n^0, p^0) \le C_0$, for all $m \in \mathbb{N}$, where $C_0 > 0$ is a constant independent of $h$.*

In addition, an optimal rate convergence analysis has been reported in [8]. Denote $(\mathsf{N}, \mathsf{P}, \Phi)$ be the exact PDE solution for the non-dimensional PNP system (1.4)–(1.6). The following regularity assumption was made for the exact solution:

$$\mathsf{N}, \mathsf{P} \in \mathcal{R} := H^4\left(0,T; C_{\text{per}}(\Omega)\right) \cap H^3\left(0,T; C_{\text{per}}^2(\Omega)\right) \cap L^\infty\left(0,T; C_{\text{per}}^6(\Omega)\right). \tag{2.21}$$

More importantly, the following separation property is assumed for the exact solution:

$$\mathsf{N} \ge \epsilon_0, \quad \mathsf{P} \ge \epsilon_0, \quad \text{for some } \epsilon_0 > 0, \quad \text{at a point-wise level.} \tag{2.22}$$

Meanwhile, the (spatial) Fourier projection of the exact solution is introduced, $\mathsf{N}_N(\cdot,t) := \mathcal{P}_N\mathsf{N}(\cdot,t)$, $\mathsf{P}_N(\cdot,t) := \mathcal{P}_N\mathsf{P}(\cdot,t)$, with the projection into $\mathcal{B}^K$, the space of trigonometric polynomials of degree to and including $K$ (with $N = 2K+1$). Of course, the projection approximation estimate is standard:

$$\|\mathsf{N}_N - \mathsf{N}\|_{L^\infty(0,T;H^k)} \le Ch^{\ell-k}\|\mathsf{N}\|_{L^\infty(0,T;H^\ell)}, \quad \|\mathsf{P}_N - \mathsf{P}\|_{L^\infty(0,T;H^k)} \le Ch^{\ell-k}\|\mathsf{P}\|_{L^\infty(0,T;H^\ell)}, \tag{2.23}$$

for any $0 \le k \le \ell$, provided that $(\mathsf{N}, \mathsf{P}) \in L^\infty(0,T; H_{\text{per}}^\ell(\Omega))$. In addition, denote $\mathsf{N}_N^m = \mathsf{N}_N(\cdot, t_m)$, $\mathsf{P}_N^m = \mathsf{P}_N(\cdot, t_m)$, with $t_m = m\cdot\Delta t$. Since $(\mathsf{N}_N, \mathsf{P}_N) \in \mathcal{B}^K$, The mass conservative property has been proved for $\mathsf{N}_N$ and $\mathsf{P}_N$ at the discrete level:

$$\overline{\mathsf{N}_N^m} = \overline{\mathsf{N}_N^{m-1}}, \quad \overline{\mathsf{P}_N^m} = \overline{\mathsf{P}_N^{m-1}}, \quad \forall m \in \mathbb{N}. \tag{2.24}$$

Meanwhile, a similar property for the numerical solution of (2.8)–(2.9) is given by (2.12). In turn, the mass conservative projection for the initial data is taken: $n^0 = \mathcal{P}_h\mathsf{N}_N(\cdot, t=0)$, $p^0 = \mathcal{P}_h\mathsf{P}_N(\cdot, t=0)$:

$$(n^0)_{i,j,k} := \mathsf{N}_N(p_i, p_j, p_k, t=0), \quad (p^0)_{i,j,k} := \mathsf{P}_N(p_i, p_j, p_k, t=0). \tag{2.25}$$

Similarly, for the exact electric potential $\Phi$, its Fourier projection is denoted as $\Phi_N$. Subsequently, the error grid function is defined as

$$e_n^m := \mathcal{P}_h\mathsf{N}_N^m - n^m, \quad e_p^m := \mathcal{P}_h\mathsf{P}_N^m - p^m, \quad e_\phi^m := \mathcal{P}_h\Phi_N^m - \phi^m, \quad \forall\, m \in \mathbb{N}. \tag{2.26}$$

Because of the fact that $\overline{e_n^m} = \overline{e_p^m} = 0$, for any $m \geq 0$, we see that the discrete norm $\|\cdot\|_{-1,h}$ is well defined for the error grid function.

The convergence result of the proposed numerical scheme is stated in the following theorem.

**Theorem 2.3** (*[8]*). *Given initial data* $\mathsf{N}(\cdot, t=0), \mathsf{P}(\cdot, t=0) \in C^6_{\text{per}}(\Omega)$, *suppose the exact solution for the PNP system (1.4)–(1.5) is of regularity class* $\mathcal{R}$. *Then, provided* $\Delta t$ *and* $h$ *are sufficiently small, and under the linear refinement requirement* $C_1 h \leq \Delta t \leq C_2 h$, *we have*

$$\|e_n^m\|_2 + \|e_p^m\|_2 + \Big(\Delta t \sum_{k=1}^{m} (\|\nabla_h e_n^k\|_2^2 + \|\nabla_h e_p^k\|_2^2)\Big)^{1/2} + \|e_\phi^m\|_{H_h^2} \leq C(\Delta t + h^2), \tag{2.27}$$

*for all positive integers* $m$, *such that* $t_m = m\Delta t \leq T$, *where* $C > 0$ *is independent of* $\Delta t$ *and* $h$.

In fact, in the convergence analysis, a few supplementary fields, $\mathsf{N}_{\Delta t,1}$, $\mathsf{N}_{\Delta t,2}$, $\mathsf{P}_{\Delta t,1}$, $\mathsf{P}_{\Delta t,2}$ and $\check{\mathsf{N}}$, $\check{\mathsf{P}}$, have been constructed:

$$\check{\mathsf{N}} = \mathsf{N}_N + \mathcal{P}_N(\Delta t \mathsf{N}_{\Delta t,1} + \Delta t^2 \mathsf{N}_{\Delta t,2} + h^2 \mathsf{N}_{h,1}), \quad \check{\mathsf{P}} = \mathsf{P}_N + \mathcal{P}_N(\Delta t \mathsf{P}_{\Delta t,1} + \Delta t^2 \mathsf{P}_{\Delta t,2} + h^2 \mathsf{P}_{h,1}), \tag{2.28}$$

so that a higher $O(\Delta t^3 + h^4)$ consistency is satisfied with the given numerical scheme (2.8)–(2.11). These constructed profiles depend solely on the exact solution $(\mathsf{N}, \mathsf{P})$.

In turn, alternate numerical error functions have been introduced:

$$\tilde{n}^m := \mathcal{P}_h \check{\mathsf{N}}^m - n^m, \quad \tilde{p}^m := \mathcal{P}_h \check{\mathsf{P}}^m - p^m, \quad \tilde{\phi}^m := (-\Delta_h)^{-1}(\tilde{p}^m - \tilde{n}^m), \quad \forall\, m \in \mathbb{N}. \tag{2.29}$$

Finally, the following convergence estimate has been derived in [8]:

$$\|\tilde{n}^{m+1}\|_2 + \|\tilde{p}^{m+1}\|_2 + \Big(\Delta t \sum_{k=1}^{m+1} (\|\nabla_h \tilde{n}^k\|_2^2 + \|\nabla_h \tilde{p}^k\|_2^2)\Big)^{1/2} \leq C(\Delta t^3 + h^4). \tag{2.30}$$

As a result of the convergence estimate (with higher order asymptotic expansion in $\check{\mathsf{N}}$ and $\check{\mathsf{P}}$), an application of an inverse inequality leads to

$$\|\tilde{n}^k\|_\infty + \|\tilde{p}^k\|_\infty \leq \frac{C\|\tilde{n}^k\|_2 + \|\tilde{p}^k\|_2}{h^{3/2}} \leq \frac{C(\Delta t^3 + h^4)}{h^{3/2}} \leq C(\Delta t^{3/2} + h^{5/2}) \leq \Delta t, \tag{2.31}$$

for any $k \geq 0$, under the linear refinement requirement $C_1 h \leq \Delta t \leq C_2 h$. Furthermore, the following $\|\cdot\|_\infty$ estimate for the discrete temporal difference of the numerical solution could be derived:

$$\begin{aligned} &\|n^{m+1} - n^m\|_\infty \leq \|\check{\mathsf{N}}^{m+1} - \check{\mathsf{N}}^m\|_\infty + \|\tilde{n}^{m+1} - \tilde{n}^m\|_\infty \leq C\Delta t + \Delta t = C_3 \Delta t, \\ &\|p^{m+1} - p^m\|_\infty \leq C_3 \Delta t, \quad \text{(similar analysis)}, \end{aligned} \tag{2.32}$$

where the inequality $\|\check{\mathsf{N}}^{m+1} - \check{\mathsf{N}}^m\|_\infty \leq C\Delta t$ comes from the $C^1(0, T; C^0)$ regularity of $\check{\mathsf{N}}$.

With the help of the $\|\cdot\|_\infty$ bound (2.31) of the numerical error functions, the following bounds become available

$$\frac{\epsilon_0}{2} \leq n^k, p^k \leq C_4 + 1 =: C_5, \quad \text{at a point-wise level, for any } k \geq 0, \tag{2.33}$$

provided that $\Delta t$ and $h$ are sufficiently small. In fact, such a derivation is based on the uniform-in-time $\|\cdot\|_\infty$ bound of the constructed profiles, $\|\check{\mathsf{N}}\|_\infty, \|\check{\mathsf{P}}\|_\infty \leq C_4$, as well as the separation properties, $\check{\mathsf{N}}, \check{\mathsf{P}} \geq \frac{5\epsilon_0}{8}$.

## 3. The iteration solver and the convergence analysis

Of course, an iteration solver is needed to implement the fully nonlinear scheme (2.8)–(2.11) at each time step. A method was proposed in [8] and is recounted here. First, the initial value for the nonlinear iteration is taken as $n^{(0)} := n^m$, $p^{(0)} := p^m$, and $\phi^{(0)} := \phi^m$. Subsequently, given the $k$th iterates, $n^{(k)}$, $p^{(k)}$, $\phi^{(k)}$, we obtain the $k+1$st iterate by solving the following system:

$$\begin{aligned} &\frac{n^{(k+1)} - n^m}{\Delta t} - \nabla_h \cdot \Big(\check{\mathcal{M}}_n^m \nabla_h \Big(\frac{n^{(k+1)} - n^{(k)}}{n^{(k)}}\Big)\Big) = \nabla_h \cdot \Big(\check{\mathcal{M}}_n^m \nabla_h \Big(\ln n^{(k)} - \phi^{(k)}\Big)\Big), \\ &\frac{p^{(k+1)} - p^m}{\Delta t} - \nabla_h \cdot \Big(\check{\mathcal{M}}_p^m \nabla_h \Big(\frac{p^{(k+1)} - p^{(k)}}{p^{(k)}}\Big)\Big) = \nabla_h \cdot \Big(\check{\mathcal{M}}_p^m \nabla_h \Big(\ln p^{(k)} + \phi^{(k)}\Big)\Big), \\ &-\Delta_h \phi^{(k+1)} = p^{(k+1)} - n^{(k+1)}. \end{aligned} \tag{3.1}$$

The point-wise positivity of $\check{\mathcal{M}}_n^m$ and $\check{\mathcal{M}}_p^m$ has been justified by the positivity-preserving analysis. In fact, the unique solvability of the linear elliptic system (3.1), in the divergence form, can be theoretically ensured, provided that the point-wise positivity of the iteration solution $n^{(k)}$ and $p^{(k)}$ is available. The system (3.1) makes use of a Newton linearization

with respect to the logarithmic nonlinear parts: for any $a, b > 0$,

$$\ln(a) = \ln(b) + \frac{a-b}{b} - \frac{1}{2}\frac{(a-b)^2}{\zeta^2}, \tag{3.2}$$

for some $\zeta$ between $a$ and $b$. In addition, we observe that

$$\overline{n^{(k+1)}} = \overline{n^{(k)}} = \overline{n^m}, \quad \overline{p^{(k+1)}} = \overline{p^{(k)}} = \overline{p^m}, \quad \overline{n^m} = \overline{p^m}, \tag{3.3}$$

so that $\mathcal{L}_{\breve{\mathcal{M}}_n^m}(n^{(k+1)} - n^m)$, $\mathcal{L}_{\breve{\mathcal{M}}_p^m}(p^{(k+1)} - p^m)$, as well as $(-\Delta_h)^{-1}(p^{(k+1)} - n^{(k+1)})$, are well defined.

Given the numerical solution $(n^m, p^m)$ at the previous time step $t^m$, and we assume that the numerical scheme (2.8)–(2.11) has been exactly implemented up to time step $t^m$. As a result of the point-wise bound (2.33) of $n^m$ and $p^m$, the following lower and upper bounds for $\breve{\mathcal{M}}_n^m$ and $\breve{\mathcal{M}}_p^m$ are straightforward:

$$\frac{\epsilon_0}{2} \le \breve{\mathcal{M}}_n^m \le C_4 + 1 = C_5, \quad \frac{D\epsilon_0}{2} \le \breve{\mathcal{M}}_p^m \le DC_5, \quad \text{at a point-wise level.} \tag{3.4}$$

We introduce the following iteration error functions:

$$\hat{e}_n^{(k)} = n^{m+1} - n^{(k)}, \quad \hat{e}_p^{(k)} = p^{m+1} - p^{(k)}, \quad \hat{e}_\phi^{(k)} = \phi^{m+1} - \phi^{(k)}. \tag{3.5}$$

By the fact that $\overline{n^{m+1}} = \overline{n^m}$, $\overline{p^{m+1}} = \overline{p^m}$, and $\overline{n^m} = \overline{p^m}$, we see that

$$\overline{\hat{e}_n^{(k)}} = \overline{\hat{e}_p^{(k)}} = 0, \quad \forall k \ge 0, \tag{3.6}$$

so that $\mathcal{L}_{\breve{\mathcal{M}}_n^m}(\hat{e}_n^{(k+1)})$, $\mathcal{L}_{\breve{\mathcal{M}}_p^m}(\hat{e}_p^{(k+1)})$, as well as $(-\Delta_h)^{-1}(\hat{e}_p^{(k)} - \hat{e}_n^{(k)})$, are well defined. Finally, the following weighed numerical "error energy" is defined:

$$F^{(k)} := \frac{\epsilon_0}{4C_5^2\Delta t}\left(\|\hat{e}_n^{(k)}\|_{-1,h}^2 + \|\hat{e}_p^{(k)}\|_{-1,h}^2\right) + \frac{1}{2(C_5+1)}\left(\|\hat{e}_n^{(k)}\|_2^2 + \|\hat{e}_p^{(k)}\|_2^2\right). \tag{3.7}$$

The main theoretical result of this article is stated in the following theorem.

**Theorem 3.1.** *Given the numerical solution $n^m$, $p^m$ and $\phi^m = (-\Delta_h)^{-1}(p^m - n^m)$ at the previous time step. Then, provided $\Delta t$ and $h$ are sufficiently small, and under the linear refinement requirement $C_1 h \le \Delta t \le C_2 h$, the following estimates hold:*

$$F^{(1)} \le C_6 \Delta t^2 F^{(0)}, \tag{3.8}$$

$$F^{(2)} \le C_7 \Delta t F^{(1)}, \tag{3.9}$$

$$F^{(k+1)} \le C_8 \Delta t^2 F^{(k)}, \quad \forall\, k \ge 2, \tag{3.10}$$

*where $C_6$, $C_7$ and $C_8 > 0$ are independent of $\Delta t$ and $h$.*

**Proof.** First we make an a-priori assumption:

$$\frac{\epsilon_0}{4} \le n^{(k)},\ p^{(k)} \le C_5 + 1, \quad \text{at a point-wise level.} \tag{3.11}$$

This a-priori assumption will be recovered by the convergence analysis at the next iteration stage. With such an assumption, the iteration algorithm (3.1) is well-defined.

Subtracting the iteration algorithm (3.1) from the exact numerical solution (2.8)–(2.11) gives

$$\begin{aligned}
\frac{\hat{e}_n^{(k+1)}}{\Delta t} &= \nabla_h \cdot \left(\breve{\mathcal{M}}_n^m \nabla_h \left(\ln n^{m+1} - \ln n^{(k)} - \frac{n^{(k+1)} - n^{(k)}}{n^{(k)}} + (-\Delta_h)^{-1}(\hat{e}_n^{(k)} - \hat{e}_p^{(k)})\right)\right), \\
\frac{\hat{e}_p^{(k+1)}}{\Delta t} &= \nabla_h \cdot \left(\breve{\mathcal{M}}_p^m \nabla_h \left(\ln p^{m+1} - \ln p^{(k)} - \frac{p^{(k+1)} - p^{(k)}}{p^{(k)}} + (-\Delta_h)^{-1}(\hat{e}_p^{(k)} - \hat{e}_n^{(k)})\right)\right).
\end{aligned} \tag{3.12}$$

In fact, such an error system could be rewritten as

$$\begin{aligned}
&\frac{1}{\Delta t}\mathcal{L}_{\breve{\mathcal{M}}_n^m}(\hat{e}_n^{(k+1)}) + \ln n^{m+1} - \ln n^{(k)} - \frac{n^{(k+1)} - n^{(k)}}{n^{(k)}} + (-\Delta_h)^{-1}(\hat{e}_n^{(k)} - \hat{e}_p^{(k)}) = 0, \\
&\frac{1}{\Delta t}\mathcal{L}_{\breve{\mathcal{M}}_p^m}(\hat{e}_p^{(k+1)}) + \ln p^{m+1} - \ln p^{(k)} - \frac{p^{(k+1)} - p^{(k)}}{p^{(k)}} + (-\Delta_h)^{-1}(\hat{e}_p^{(k)} - \hat{e}_n^{(k)}) = 0.
\end{aligned} \tag{3.13}$$

Next we look at the first equation in (3.13), the error equation for $\hat{e}_n^{(k+1)}$. An application of Taylor's Theorem reveals that

$$\ln n^{m+1} - \ln n^{(k)} = \frac{1}{\xi_n^{(k)}}\hat{e}_n^{(k)}, \tag{3.14}$$

for some $\xi_n^{(k)}$ between $n^{m+1}$ and $n^{(k)}$ in a point-wise sense. Since $\xi_n^{(k)}$ is "between" $n^{m+1}$ and $n^{(k)}$, we conclude that

$$|\xi_n^{(k)} - n^{(k)}| \leq |n^{m+1} - n^{(k)}| \leq |\hat{e}_n^{(k)}|,$$

so that

$$\|\xi_n^{(k)} - n^{(k)}\|_\infty \leq \|\hat{e}_n^{(k)}\|_\infty. \tag{3.15}$$

Because of the separation properties and upper bounds satisfied by both $n^{m+1}$ and $n^{(k)}$ – see (2.33) and (3.11), respectively – the following estimate is valid for $\xi_n^{(k)}$:

$$\frac{\epsilon_0}{4} \leq \xi_n^{(k)} \leq C_5 + 1, \quad \text{at a point-wise level.} \tag{3.16}$$

Meanwhile, for the term $n^{(k+1)} - n^{(k)}$, we have

$$n^{(k+1)} - n^{(k)} = (n^{m+1} - \hat{e}_n^{(k+1)}) - (n^{m+1} - \hat{e}_n^{(k)}) = -(\hat{e}_n^{(k+1)} - \hat{e}_n^{(k)}). \tag{3.17}$$

Therefore, the error equation for $\hat{e}_n^{(k+1)}$ could be reformulated as

$$\frac{1}{\Delta t}\mathcal{L}_{\check{\mathcal{M}}_n^m}(\hat{e}_n^{(k+1)}) + \frac{1}{\xi_n^{(k)}}\hat{e}_n^{(k)} + \frac{\hat{e}_n^{(k+1)} - \hat{e}_n^{(k)}}{n^{(k)}} + (-\Delta_h)^{-1}(\hat{e}_n^{(k)} - \hat{e}_p^{(k)}) = 0. \tag{3.18}$$

The two nonlinear iteration error terms can be rewritten as

$$\frac{1}{\xi_n^{(k)}}\hat{e}_n^{(k)} + \frac{\hat{e}_n^{(k+1)} - \hat{e}_n^{(k)}}{n^{(k)}} = \frac{n^{(k)} - \xi_n^{(k)}}{\xi_n^{(k)} n^{(k)}}\hat{e}_n^{(k)} + \frac{\hat{e}_n^{(k+1)}}{n^{(k)}}. \tag{3.19}$$

Next, define

$$\zeta_n^{(k)} := \frac{n^{(k)} - \xi_n^{(k)}}{\xi_n^{(k)}}.$$

Then, the point-wise inequality (3.15) implies that

$$|\zeta_n^{(k)}| = \frac{|n^{(k)} - \xi_n^{(k)}|}{\xi_n^{(k)}} \leq \frac{|\hat{e}_n^{(k)}|}{\xi_n^{(k)}} \leq 4\epsilon_0^{-1}|\hat{e}_n^{(k)}|, \tag{3.20}$$

in which the bound (3.16) has been applied in the last step. Going back (3.18), we get

$$\frac{1}{\Delta t}\mathcal{L}_{\check{\mathcal{M}}_n^m}(\hat{e}_n^{(k+1)}) + \frac{\hat{e}_n^{(k+1)}}{n^{(k)}} = -\frac{\zeta_n^{(k)}}{n^{(k)}}\hat{e}_n^{(k)} + (-\Delta_h)^{-1}(\hat{e}_n^{(k)} - \hat{e}_p^{(k)}). \tag{3.21}$$

Next, taking a discrete inner product of (3.21) with $\hat{e}_n^{(k+1)}$ gives

$$\frac{1}{\Delta t}\|\hat{e}_n^{(k+1)}\|^2_{\mathcal{L}^{-1}_{\check{\mathcal{M}}_n^m}} + \left\langle \frac{1}{n^{(k)}}, (\hat{e}_n^{(k+1)})^2 \right\rangle_\Omega = -\left\langle \frac{\zeta_n^{(k)}}{n^{(k)}}, \hat{e}_n^{(k)}\hat{e}_n^{(k+1)} \right\rangle_\Omega + \langle \hat{e}_n^{(k+1)}, \hat{e}_n^{(k)} - \hat{e}_p^{(k)} \rangle_{-1,h}. \tag{3.22}$$

For the first term on the left hand side, an application of Lemma 2.2 reveals that

$$\|\hat{e}_n^{(k+1)}\|^2_{\mathcal{L}^{-1}_{\check{\mathcal{M}}_n^m}} \geq \frac{\epsilon_0}{2C_5^2}\|\hat{e}_n^{(k+1)}\|^2_{-1,h}, \tag{3.23}$$

with the estimate (2.33) applied. The lower bound of the nonlinear inner product on the left hand side could be obtained with the help of the a-priori assumption (3.11):

$$\left\langle \frac{1}{n^{(k)}}, (\hat{e}_n^{(k+1)})^2 \right\rangle_\Omega \geq \frac{1}{C_5 + 1}\|\hat{e}_n^{(k+1)}\|_2^2. \tag{3.24}$$

For the term associated with the electric potential, a direct application of the Cauchy–Schwarz and Young inequalities gives

$$\begin{aligned} \langle \hat{e}_n^{(k+1)}, \hat{e}_n^{(k)} - \hat{e}_p^{(k)} \rangle_{-1,h} &\leq \|\hat{e}_n^{(k+1)}\|_{-1,h} \cdot \|\hat{e}_n^{(k)} - \hat{e}_p^{(k)}\|_{-1,h} \\ &\leq \frac{\epsilon_0}{4C_5^2\Delta t}\|\hat{e}_n^{(k+1)}\|^2_{-1,h} + C_5^2\epsilon_0^{-1}\Delta t\|\hat{e}_n^{(k)} - \hat{e}_p^{(k)}\|^2_{-1,h}. \end{aligned} \tag{3.25}$$

For the nonlinear error inner product on the right hand side of (3.22), a more careful calculation reveals that

$$\begin{aligned} -\left\langle \frac{\zeta_n^{(k)}}{n^{(k)}}, \hat{e}_n^{(k)}\hat{e}_n^{(k+1)} \right\rangle_\Omega &\le \frac{1}{2}\left\langle \frac{1}{n^{(k)}}, (\hat{e}_n^{(k+1)})^2 \right\rangle_\Omega + \frac{1}{2}\left\langle \frac{1}{n^{(k)}}, (\zeta_n^{(k)})^2(\hat{e}_n^{(k)})^2 \right\rangle_\Omega \\ &\le \frac{1}{2}\left\langle \frac{1}{n^{(k)}}, (\hat{e}_n^{(k+1)})^2 \right\rangle_\Omega + \frac{1}{2}\cdot 4\epsilon_0^{-1}\cdot 16\epsilon_0^{-2}\|\hat{e}_n^{(k)}\|_\infty^2\cdot\|\hat{e}_n^{(k)}\|_2^2 \\ &\le \frac{1}{2}\left\langle \frac{1}{n^{(k)}}, (\hat{e}_n^{(k+1)})^2 \right\rangle_\Omega + 32\epsilon_0^{-3}\|\hat{e}_n^{(k)}\|_\infty^2\cdot\|\hat{e}_n^{(k)}\|_2^2. \end{aligned} \tag{3.26}$$

Therefore, a substitution of (3.23)–(3.26) into (3.22) leads to

$$\begin{aligned} &\frac{\epsilon_0}{4C_5^2\Delta t}\|\hat{e}_n^{(k+1)}\|_{-1,h}^2 + \frac{1}{2(C_5+1)}\|\hat{e}_n^{(k+1)}\|_2^2 \\ &\quad\le C_5^2\epsilon_0^{-1}\Delta t\|\hat{e}_n^{(k)} - \hat{e}_p^{(k)}\|_{-1,h}^2 + 32\epsilon_0^{-3}\|\hat{e}_n^{(k)}\|_\infty^2\cdot\|\hat{e}_n^{(k)}\|_2^2. \end{aligned} \tag{3.27}$$

Similarly, the second equation in (3.13), the error equation for $\hat{e}_p^{(k+1)}$, could be reformulated as

$$\frac{1}{\Delta t}\mathcal{L}_{\check{\mathcal{M}}_p^m}(\hat{e}_p^{(k+1)}) + \frac{1}{\xi_p^{(k)}}\hat{e}_p^{(k)} + \frac{\hat{e}_p^{(k+1)} - \hat{e}_p^{(k)}}{p^{(k)}} + (-\Delta_h)^{-1}(\hat{e}_p^{(k)} - \hat{e}_n^{(k)}) = 0, \tag{3.28}$$

where $\xi_p^{(k)}$ is between $p^{m+1}$ and $p^{(k)}$ and satisfies

$$|\zeta_p^{(k)}| \le 4\epsilon_0^{-1}|\hat{e}_p^{(k)}|.$$

The error equation for $p$ can be further rewritten as

$$\frac{1}{\Delta t}\mathcal{L}_{\check{\mathcal{M}}_p^m}(\hat{e}_p^{(k+1)}) + \frac{\hat{e}_p^{(k+1)}}{p^{(k)}} = -\frac{\zeta_p^{(k)}}{p^{(k)}}\hat{e}_p^{(k)} + (-\Delta_h)^{-1}(\hat{e}_p^{(k)} - \hat{e}_n^{(k)}). \tag{3.29}$$

In addition, taking a discrete inner product of (3.21) with $\hat{e}_p^{(k+1)}$, we are able to derive the following iteration error estimate

$$\begin{aligned} &\frac{\epsilon_0}{4C_5^2\Delta t}\|\hat{e}_p^{(k+1)}\|_{-1,h}^2 + \frac{1}{2(C_5+1)}\|\hat{e}_p^{(k+1)}\|_2^2 \\ &\quad\le C_5^2\epsilon_0^{-1}\Delta t\|\hat{e}_n^{(k)} - \hat{e}_p^{(k)}\|_{-1,h}^2 + 32\epsilon_0^{-3}\|\hat{e}_p^{(k)}\|_\infty^2\cdot\|\hat{e}_p^{(k)}\|_2^2. \end{aligned} \tag{3.30}$$

The technical details are left to interested readers. Finally, a combination of (3.27) and (3.30) yields

$$\begin{aligned} &\frac{\epsilon_0}{4C_5^2\Delta t}(\|\hat{e}_n^{(k+1)}\|_{-1,h}^2 + \|\hat{e}_p^{(k+1)}\|_{-1,h}^2) + \frac{1}{2(C_5+1)}\left(\|\hat{e}_n^{(k+1)}\|_2^2 + \|\hat{e}_p^{(k+1)}\|_2^2\right) \\ &\quad\le 2C_5^2\epsilon_0^{-1}\Delta t\|\hat{e}_n^{(k)} - \hat{e}_p^{(k)}\|_{-1,h}^2 + 32\epsilon_0^{-3}\left(\|\hat{e}_n^{(k)}\|_\infty^2\cdot\|\hat{e}_n^{(k)}\|_2^2 + \|\hat{e}_p^{(k)}\|_\infty^2\cdot\|\hat{e}_p^{(k)}\|_2^2\right) \\ &\quad\le 4C_5^2\epsilon_0^{-1}\Delta t\left(\|\hat{e}_n^{(k)}\|_{-1,h}^2 + \|\hat{e}_p^{(k)}\|_{-1,h}^2\right) + 32\epsilon_0^{-3}\left(\|\hat{e}_n^{(k)}\|_\infty^2\cdot\|\hat{e}_n^{(k)}\|_2^2 + \|\hat{e}_p^{(k)}\|_\infty^2\cdot\|\hat{e}_p^{(k)}\|_2^2\right). \end{aligned} \tag{3.31}$$

### 3.1. Iteration stage 1: $k = 0$

At $k = 0$, we see that the preliminary error estimate (2.32) (for the exact solution of (2.8)–(2.11)) implies that

$$\|\hat{e}_n^{(0)}\|_\infty = \|n^{m+1} - n^m\|_\infty \le C_3\Delta t, \quad \|\hat{e}_p^{(0)}\|_\infty = \|p^{m+1} - p^m\|_\infty \le C_3\Delta t, \tag{3.32}$$

due to initializations $n^{m+1,(0)} = n^m$, $p^{m+1,(0)} = p^m$. A substitution of the last inequality into (3.31) leads to the following iteration error estimate for $k = 0$:

$$\begin{aligned} &\frac{\epsilon_0}{4C_5^2\Delta t}(\|\hat{e}_n^{(1)}\|_{-1,h}^2 + \|\hat{e}_p^{(1)}\|_{-1,h}^2) + \frac{1}{2(C_5+1)}(\|\hat{e}_n^{(1)}\|_2^2 + \|\hat{e}_p^{(1)}\|_2^2) \\ &\quad\le 4C_5^2\epsilon_0^{-1}\Delta t(\|\hat{e}_n^{(0)}\|_{-1,h}^2 + \|\hat{e}_p^{(0)}\|_{-1,h}^2) + 32C_3^2\epsilon_0^{-3}\Delta t^2(\|\hat{e}_n^{(0)}\|_2^2 + \|\hat{e}_p^{(0)}\|_2^2). \end{aligned} \tag{3.33}$$

Consequently, we get inequality (3.8), by taking

$$C_6 = \max\left(16C_5^4\epsilon_0^{-2}, 64C_3^2(C_5+1)\epsilon_0^{-3}\right).$$

### 3.2. Iteration stage 2: $k = 1$

The iteration error estimate (3.8) for $k = 0$ indicates that

$$\begin{aligned} F^{(1)} &= \frac{\epsilon_0}{4C_5^2\Delta t}(\|\hat{e}_n^{(1)}\|_{-1,h}^2 + \|\hat{e}_p^{(1)}\|_{-1,h}^2) + \frac{1}{2(C_5+1)}(\|\hat{e}_n^{(1)}\|_2^2 + \|\hat{e}_p^{(1)}\|_2^2) \\ &\le C_6\Delta t^2 F^{(0)} \\ &\le C_9C_6\Delta t^4, \end{aligned} \tag{3.34}$$

since $F^{(0)} \le C_9\Delta t^2$, which comes from the preliminary error estimate (3.32). Therefore,

$$\|\hat{e}_n^{(1)}\|_2,\ \|\hat{e}_p^{(1)}\|_2 \le C_{10}\Delta t^2, \quad C_{10} := (2C_9C_6(C_5+1))^{1/2}. \tag{3.35}$$

Subsequently, an application of an inverse inequality gives

$$\|\hat{e}_n^{(1)}\|_\infty \le \frac{C\|\hat{e}_n^{(1)}\|_2}{h^{3/2}} \le \frac{CC_{10}\Delta t^2}{h^{3/2}} \le C_{11}\Delta t^{1/2}, \quad \|\hat{e}_p^{(1)}\|_\infty \le C_{11}\Delta t^{1/2}, \ \text{(similarly)}, \tag{3.36}$$

with $C_{11} = CC_{10}$, where the linear refinement constraint, $C_1h \le \Delta t \le C_2h$, has been applied. A substitution of the last inequalities into (3.31) leads to the following iteration error estimate for $k = 1$:

$$\begin{aligned} &\frac{\epsilon_0}{4C_5^2\Delta t}(\|\hat{e}_n^{(2)}\|_{-1,h}^2 + \|\hat{e}_p^{(2)}\|_{-1,h}^2) + \frac{1}{2(C_5+1)}(\|\hat{e}_n^{(2)}\|_2^2 + \|\hat{e}_p^{(2)}\|_2^2) \\ &\quad \le 4C_5^2\epsilon_0^{-1}\Delta t(\|\hat{e}_n^{(1)}\|_{-1,h}^2 + \|\hat{e}_p^{(1)}\|_{-1,h}^2) + 32C_{11}^2\epsilon_0^{-3}\Delta t(\|\hat{e}_n^{(1)}\|_2^2 + \|\hat{e}_p^{(1)}\|_2^2), \end{aligned} \tag{3.37}$$

so that inequality (3.9) is valid, by taking

$$C_7 = \max\Big(16C_5^4\epsilon_0^{-2}, 64C_{11}^2(C_5+1)\epsilon_0^{-3}\Big).$$

### 3.3. Iteration stage 3: $k = 2$

The iteration error estimate (3.9) for $k = 1$ indicates that

$$\begin{aligned} F^{(2)} &= \frac{\epsilon_0}{4C_5^2\Delta t}(\|\hat{e}_n^{(2)}\|_{-1,h}^2 + \|\hat{e}_p^{(2)}\|_{-1,h}^2) + \frac{1}{2(C_5+1)}(\|\hat{e}_n^{(2)}\|_2^2 + \|\hat{e}_p^{(2)}\|_2^2) \\ &\le C_7\Delta t F^{(1)} \\ &\le C_9C_6C_7\Delta t^5. \end{aligned} \tag{3.38}$$

Therefore,

$$\|\hat{e}_n^{(2)}\|_2,\ \|\hat{e}_p^{(2)}\|_2 \le C_{12}\Delta t^{5/2}, \quad C_{12} = (2(C_5+1)C_9C_6C_7)^{1/2}. \tag{3.39}$$

In turn, an application of an inverse inequality leads to

$$\|\hat{e}_n^{(2)}\|_\infty \le \frac{C\|\hat{e}_n^{(2)}\|_2}{h^{3/2}} \le \frac{CC_{12}\Delta t^{5/2}}{h^{3/2}} \le C_{13}\Delta t, \quad \|\hat{e}_p^{(2)}\|_\infty \le C_{13}\Delta t, \ \text{(similar argument)}, \tag{3.40}$$

with $C_{13} = CC_{12}$. A substitution of the last inequalities into (3.31) leads to the following iteration error estimate for $k = 2$:

$$\begin{aligned} &\frac{\epsilon_0}{4C_5^2\Delta t}(\|\hat{e}_n^{(3)}\|_{-1,h}^2 + \|\hat{e}_p^{(3)}\|_{-1,h}^2) + \frac{1}{2(C_5+1)}(\|\hat{e}_n^{(3)}\|_2^2 + \|\hat{e}_p^{(3)}\|_2^2) \\ &\quad \le 4C_5^2\epsilon_0^{-1}\Delta t(\|\hat{e}_n^{(2)}\|_{-1,h}^2 + \|\hat{e}_p^{(2)}\|_{-1,h}^2) + 32C_{13}^2\epsilon_0^{-3}\Delta t^2(\|\hat{e}_n^{(2)}\|_2^2 + \|\hat{e}_p^{(2)}\|_2^2), \end{aligned} \tag{3.41}$$

so that inequality (3.10) is valid, by taking

$$C_8 = \max\Big(16C_5^4\epsilon_0^{-2}, 64C_{13}^2(C_5+1)\epsilon_0^{-3}\Big).$$

### 3.4. Higher iteration stages: $k \ge 3$

Assume that inequality (3.10) is valid up to the $k-1$st stage. Then we get

$$\begin{aligned} F^{(k)} &= \frac{\epsilon_0}{4C_5^2\Delta t}(\|\hat{e}_n^{(k)}\|_{-1,h}^2 + \|\hat{e}_p^{(k)}\|_{-1,h}^2) + \frac{1}{2(C_5+1)}(\|\hat{e}_n^{(k)}\|_2^2 + \|\hat{e}_p^{(k)}\|_2^2) \\ &\le C_8\Delta t^2 F^{(k-1)} \\ &\le \tilde{C}C_6C_7C_8\Delta t^7 \\ &\le \Delta t^6. \end{aligned} \tag{3.42}$$

Therefore,

$$\|\hat{e}_n^{(k)}\|_2,\ \|\hat{e}_p^{(k)}\|_2 \le \Delta t^3. \tag{3.43}$$

provided that $\Delta t$ is sufficiently small. In turn, an application of an inverse inequality leads to

$$\|\hat{e}_n^{(k)}\|_\infty \le \frac{C\|\hat{e}_n^{(k)}\|_2}{h^{3/2}} \quad \|\hat{e}_p^{(k)}\|_\infty \le \Delta t, \ \text{(similar argument)}. \tag{3.44}$$

Again, a substitution of the last inequalities into (3.31) leads to the following iteration error estimate for $k \ge 3$:

$$\begin{aligned} &\frac{\epsilon_0}{4C_5^2\Delta t}(\|\hat{e}_n^{(k+1)}\|_{-1,h}^2 + \|\hat{e}_p^{(k+1)}\|_{-1,h}^2) + \frac{1}{2(C_5+1)}(\|\hat{e}_n^{(k+1)}\|_2^2 + \|\hat{e}_p^{(k+1)}\|_2^2) \\ &\quad \le 4C_5^2\epsilon_0^{-1}\Delta t(\|\hat{e}_n^{(k)}\|_{-1,h}^2 + \|\hat{e}_p^{(k)}\|_{-1,h}^2) + 32\epsilon_0^{-3}\Delta t^2(\|\hat{e}_n^{(k)}\|_2^2 + \|\hat{e}_p^{(k)}\|_2^2), \end{aligned} \tag{3.45}$$

so that inequality (3.10) is valid for $k \ge 3$, by taking

$$C_8 = \max\Big(16C_5^4\epsilon_0^{-2}, 64(C_5+1)\epsilon_0^{-3}\Big).$$

Finally, we observe that the a-priori assumption (3.11) can be recovered at the next iteration stage, by applying the $\|\cdot\|_\infty$ iteration error estimate (3.36), (3.40) and (3.44):

$$\begin{aligned} &n^{(k+1)} \ge n^{m+1} - |\hat{e}_n^{(k+1)}| \ge \frac{\epsilon_0}{2} - \frac{\epsilon_0}{4} = \frac{\epsilon_0}{4}, \\ &n^{(k+1)} \le n^{m+1} + |\hat{e}_n^{(k+1)}| \le C_5 + 1, \\ &\frac{\epsilon_0}{4} \le p^{(k+1)} \le C_5 + 1, \quad \text{(similar argument)}, \end{aligned} \tag{3.46}$$

for $k = 0$, $k = 1$ and $k \ge 2$, provided that $\Delta t$ and $h$ are sufficiently small. This finishes the proof of Theorem 3.1. □

**Remark 3.1.** From the above iteration convergence analysis, we see that

$$\|\hat{e}_n^{(0)}\|_2 = O(\Delta t),\ \ \|\hat{e}_n^{(1)}\|_2 = O(\Delta t^2),\ \ \|\hat{e}_n^{(2)}\|_2 = O(\Delta t^{5/2}),\ \ \|\hat{e}_n^{(k)}\|_2 = O(\Delta t^{k+1/2}),\ \ (k \ge 3), \tag{3.47}$$

so that the convergence is at least linear, with convergence rate in the order of $O(\Delta t)$. Extensive numerical experiments have demonstrated that, only four to five iteration stages are needed to achieve a near-machine error precision at each time step. In addition, each iteration stage corresponds to a non-constant coefficient elliptic solver, with the computational cost comparable to the standard Poisson solver. Therefore, the proposed iteration algorithm turns out to be a very efficient solver to implement the numerical scheme (2.8)–(2.11).

**Remark 3.2.** In the iteration algorithm (3.1), we treat the electric potential part explicitly in the iteration, to avoid a coupling. This approach leads to a linear convergence, with convergence rate of order $O(\Delta t)$, as stated in Theorem 3.1. Meanwhile, if such a term is treated implicitly in the iteration (which leads to a coupled system), the iteration convergence order could be further improved. In fact, a careful analysis reveals the following estimate, if the electric potential part is treated implicitly:

$$\frac{1}{2(C_5+1)}(\|\hat{e}_n^{(k+1)}\|_2^2 + \|\hat{e}_p^{(k+1)}\|_2^2) \le 32\epsilon_0^{-3}(\|\hat{e}_n^{(k)}\|_\infty^2 \cdot \|\hat{e}_n^{(k)}\|_2^2 + \|\hat{e}_p^{(k)}\|_\infty^2 \cdot \|\hat{e}_p^{(k)}\|_2^2).$$

This estimate corresponds to a quadratic convergence order in the standard Newton iteration, i.e, $\hat{e}^{(k+1)} \approx \mathcal{C}(\hat{e}^k)^2$, a faster convergence order than the one given by (3.10). However, a coupled system has to be solved in this approach, and the numerical experiments have demonstrated great efficiency advantages of the proposed iteration algorithm (3.1) over this approach.

## 4. Numerical test for the iteration solver

We perform a 2-D numerical test to demonstrate the convergence rate of the iteration algorithm (3.1). The computational box, taken as $\Omega = (0, 1)^2$, is covered by a uniform mesh with $h = 0.02$, and the time step size is chosen as $\Delta t = h$. We consider the following exact solution

$$\begin{cases} n = \mathrm{e}^{-t}\sin(2\pi x)\cos(2\pi y) + 2, \\ p = \mathrm{e}^{-t}\cos(2\pi x)\sin(2\pi y) + 2, \\ \psi = \mathrm{e}^{-t}\sin(2\pi x)\sin(2\pi y), \end{cases} \tag{4.1}$$

to the PNP system (1.4)–(1.6) with additional source terms in the NP equations. The source terms and the initial conditions are determined by the known exact solution. In fact, such a test function has been used in the existing work [8] to verify the accuracy of the numerical scheme (2.8)–(2.11), and the expected numerical accuracy in both temporal and spatial

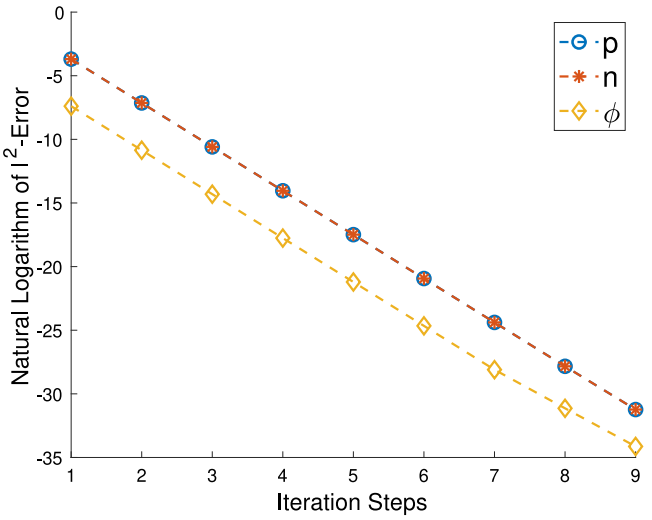


**Fig. 1.** Logarithmic plot of $\ell^2$-errors of $p$, $n$, and $\phi$ vs. iteration stages.

discretization has been reported. In this section, we focus on the convergence rate of the iteration solver (3.1) for the nonlinear discretization scheme (2.8)–(2.11).

In this test, we only focus on solving the nonlinear discretization scheme for a single time step, i.e., the first time step, and take the converged numerical solution as the reference solution. For each iteration stage, the iteration solution is compared with the reference solution. Fig. 1 displays the logarithmic plot of the $\ell^2$-error for $p$, $n$, and $\phi$ vs. the iteration stages. It is obvious that the natural logarithm of the $\ell^2$-error decreases linearly against the iteration stages, which demonstrates a linear convergence rate of the iteration algorithm (3.1) (as stated in Theorem 3.1). Therefore, this numerical test has verified the theoretical result of the linear convergence rate for the proposed iteration solver.

## 5. Concluding remarks

An iteration solver is proposed and analyzed for a finite difference scheme for the Poisson-Nernst–Planck (PNP) system, formulated in the Energetic Variational Approach (EnVarA). In the given numerical scheme, the mobility concentration function is explicitly treated to ensure the unique solvability, while both the logarithmic and the electric potential diffusion terms are treated implicitly, because of their convex natures. The positivity-preserving property for both concentrations, an unconditional energy stability, and the optimal rate error estimate have been established in a recent work. In this article, an iteration solver is proposed to implement the numerical scheme, which includes a modified Newton iteration for the nonlinear and logarithmic part, combined with a linear iteration for the electric potential part. In turn, a linear elliptic equation, in the divergence form, needs to be solved at each iteration stage. A linear convergence analysis is provided for the proposed iteration algorithm, under the separation assumption for the exact PDE solution and the numerical solution at each iteration stage. The positivity of both concentration variables at each iteration stage is crucial to ensure the well-posed property of the elliptic system. With the help of the uniform distance between the numerical solutions and the singular limit value, the singularity issue associated with the logarithmic term could be avoided in the iteration analysis, and the convex nature of the logarithmic energy functional will lead to a well-posed nonlinear error at each iteration stage. Finally, a linear convergence analysis is reported for the proposed iteration process, with convergence rate in the same order of the time step size. It will be the first such result for the highly nonlinear and singular PNP system. In addition, a numerical test has also demonstrated the linear convergence rate of the proposed iteration solver.

## Acknowledgments

This work is supported in part by the National Science Foundation (USA) grants NSF DMS-1759535, NSF DMS-1759536 (C. Liu), NSF DMS-2012669 (C. Wang), NSF DMS-1719854, DMS-2012634 (S. Wise), National Natural Science Foundation of China 11971342 (X. Yue), 12171319, Young Elite Scientist Sponsorship Program by Jiangsu Association for Science and Technology, China, Natural Science Foundation of Jiangsu Province (BK20200098), China, and National Key R&D Program of China 2018YFB0204404 (S. Zhou).

## References


[1] M.Z. Bazant, K. Thornton, A. Ajdari, Diffuse-charge dynamics in electrochemical systems, Phys. Rev. E 70 (2) (2004) 021506.
[2] Y. Ben, H.C. Chang, Nonlinear Smoluchowski slip velocity and micro-vortex generation, J. Fluid Mech. 461 (2002) 229–238.
[3] R.S. Eisenberg, Computing the field in proteins and channels, J. Mem. Biol. 150 (1996) 1–25.
[4] A. Flavell, M. Machen, R. Eisenberg, J. Kabre, C. Liu, X. Li, A conservative finite difference scheme for Poisson-Nernst-Planck equations, J. Comput. Electron. 13 (2014) 235–249.
[5] N. Gavish, A. Yochelis, Theory of phase separation and polarization for pure ionic liquids, J. Phys. Chem. Lett. 7 (2016) 1121–1126.
[6] K. Promislow, J.M. Stockie, Adiabatic relaxation of convective-diffusive gas transport in a porous fuel cell electrode, SIAM J. Appl. Math. 62 (1) (2001) 180–205.
[7] B. Eisenberg, Y. Hyon, C. Liu, Energy variational analysis of ions in water and channels: Field theory for primitive models of complex ionic fluids, J. Chem. Phys. 133 (10) (2010) 104104.
[8] C. Liu, C. Wang, S.M. Wise, X. Yue, S. Zhou, A positivity-preserving, energy stable and convergent numerical scheme for the Poisson-Nernst-Planck system, Math. Comp. 90 (2021) 2071–2106.
[9] J. Ding, Z. Wang, S. Zhou, Positivity preserving finite difference methods for Poisson-Nernst-Planck equations with steric interactions: Application to slit-shaped nanopore conductance, J. Comput. Phys. 397 (2019) 108864.
[10] J. Ding, Z. Wang, S. Zhou, Structure-preserving and efficient numerical methods for ion transport, J. Comput. Phys. 418 (2020) 109597.
[11] D. He, K. Pan, X. Yue, A positivity preserving and free energy dissipative difference scheme for the Poisson-Nernst-Planck system, J. Sci. Comput. 81 (2019) 436–458.
[12] J. Hu, X. Huang, A fully discrete positivity-preserving and energy-dissipative finite difference scheme for Poisson-Nernst-Planck equations, Numer. Math. 145 (2020) 77–115.
[13] H. Liu, Z. Wang, A free energy satisfying finite difference method for Poisson-Nernst-Planck equations, J. Comput. Phys. 268 (2014) 363–376.
[14] H. Liu, W. Maimaitiyiming, Efficient, positive and energy stable schemes for multi-d Poisson-Nernst-Planck systems, J. Sci. Comput. 87 (2021) 92.
[15] H. Liu, W. Maimaitiyiming, Unconditional positivity-preserving and energy stable schemes for a reduced Poisson-Nernst-Planck system, Commun. Comput. Phys. 27 (2020) 1505–1529.
[16] F. Siddiqua, Z. Wang, S. Zhou, A modified Poisson-Nernst-Planck model with excluded volume effect: Theory and numerical implementation, Commun. Math. Sci. 16 (2018) 251–271.
[17] A. Flavell, J. Kabre, X. Li, An energy-preserving discretization for the Poisson-Nernst-Planck equations, J. Comput. Electron 16 (2017) 431–441.
[18] H. Liu, Z. Wang, A free energy satisfying discontinuous Galerkin method for one-dimensional Poisson-Nernst-Planck systems, J. Comput. Phys. 328 (2017) 413–437.
[19] M. Metti, J. Xu, C. Liu, Energetically stable discretizations for charge transport and electrokinetic models, J. Comput. Phys. 306 (2016) 1–18.
[20] J. Ding, C. Wang, S. Zhou, Optimal rate convergence analysis of a second order numerical scheme for the Poisson-Nernst-Planck system, Numer. Math. Theory Methods Appl. 12 (2019) 607–626.
[21] H. Gao, D. He, Linearized conservative finite element methods for the Nernst-Planck-Poisson equations, J. Sci. Comput. 72 (2017) 1269–1289.
[22] A. Prohl, M. Schmuck, Convergent discretizations for the Nernst-Planck-Poisson system, Numer. Math. 111 (2009) 591–630.
[23] Y. Sun, P. Sun, B. Zheng, G. Lin, Error analysis of finite element method for Poisson-Nernst-Planck equations, J. Comput. Appl. Math. 301 (2016) 28–43.
[24] D. He, K. Pan, An energy preserving finite difference scheme for the Poisson-Nernst-Planck system, Appl. Math. Comput. 287 (2015) 214–223.
[25] M. Mirzadeh, F. Gibou, A conservative discretization of the Poisson-Nernst-Planck equations on adaptive cartesian grids, J. Comput. Phys. 274 (2014) 633–653.
[26] Y. Qian, C. Wang, S. Zhou, A positive and energy stable numerical scheme for the Poisson-Nernst-Planck-Cahn-Hilliard equations with steric interactions, J. Comput. Phys. 426 (2021) 109908.
[27] B. Tu, M. Chen, Y. Xie, L. Zhang, B. Eisenberg, B. Lu, A parallel finite element simulator for ion transport through three-dimensional ion channel systems, J. Comput. Chem. 287 (2015) 214–223.
[28] S. Xu, M. Chen, S. Majd, X. Yue, C. Liu, Modeling and simulating asymmetrical conductance changes in Gramicidin pores, Mol. Based Math. Biol. 2 (2014) 34–55.
[29] W. Chen, C. Wang, X. Wang, S.M. Wise, Positivity-preserving, energy stable numerical schemes for the Cahn-Hilliard equation with logarithmic potential, J. Comput. Phys.: X 3 (2019) 100031.
[30] L. Dong, C. Wang, H. Zhang, Z. Zhang, A positivity-preserving, energy stable and convergent numerical scheme for the Cahn-Hilliard equation with a Flory-Huggins-deGennes energy, Commun. Math. Sci. 17 (2019) 921–939.
[31] L. Dong, C. Wang, S.M. Wise, Z. Zhang, A positivity-preserving, energy stable scheme for a ternary Cahn-Hilliard system with the singular interfacial parameters, J. Comput. Phys. 442 (2021) 110451.
[32] L. Dong, C. Wang, H. Zhang, Z. Zhang, A positivity-preserving second-order BDF scheme for the Cahn-Hilliard equation with variable interfacial parameters, Commun. Comput. Phys. 28 (2020) 967–998.
[33] C. Liu, C. Wang, Y. Wang, A structure-preserving, operator splitting scheme for reaction-diffusion equations with detailed balance, J. Comput. Phys. 436 (2021) 110253.
[34] Y. Qin, C. Wang, Z. Zhang, A positivity-preserving and convergent numerical scheme for the binary fluid-surfactant system, Int. J. Numer. Anal. Model. 18 (2021) 399–425.
[35] M. Yuan, W. Chen, C. Wang, S.M. Wise, Z. Zhang, An energy stable finite element scheme for the three-component Cahn-Hilliard-type model for macromolecular microsphere composite hydrogels, J. Sci. Comput. 87 (2021) 78.
[36] J. Zhang, C. Wang, S.M. Wise, Z. Zhang, Structure-preserving, energy stable numerical schemes for a liquid thin film coarsening model, SIAM J. Sci. Comput. 43 (2) (2021) A1248–A1272.
[37] J. Guo, C. Wang, S.M. Wise, X. Yue, An $H^2$ convergence of a second-order convex-splitting, finite difference scheme for the three-dimensional Cahn-Hilliard equation, Commun. Math. Sci. 14 (2016) 489–515.
[38] C. Wang, S.M. Wise, An energy stable and convergent finite-difference scheme for the modified phase field crystal equation, SIAM J. Numer. Anal. 49 (2011) 945–969.
[39] S.M. Wise, Unconditionally stable finite difference, nonlinear multigrid simulation of the Cahn-Hilliard-Hele-Shaw system of equations, J. Sci. Comput. 44 (2010) 38–68.
[40] S.M. Wise, C. Wang, J. Lowengrub, An energy stable and convergent finite-difference scheme for the phase field crystal equation, SIAM J. Numer. Anal. 47 (2009) 2269–2288.